Compressive Failure Model for Anisotropic Plates with a Cutout

Zafer Gürdal* and Raphael T. Haftka†
Virginia Polytechnic Institute and State University, Blacksburg, Virginia

This paper introduces a failure model for laminated composite plates with a cutout under combined compressive and shear loads. The model is based on the kinking failure of the load-carrying fibers around a cutout, and includes the effect of local shearing and compressive stresses. Comparison of the predictions of the model with available experimental results for quasi-isotropic and orthotropic plates with a circular hole under pure compression indicated a good agreement. The predictions for orthotropic plates under combined loading are compared with the predictions of a point-stress model. The present model indicates significant reductions in axial load-carrying capacity due to shearing loads for plates with a principal axis of orthotropy oriented along the axial load direction. A gain in strength is achieved by rotating the axis of orthotropy to counteract the shearing stress or by restraining the compressive-shear deformation coupling.

Introduction

COMPRESSIVE failure of plates with a cutout can be modeled by considering either the strength failure or the loss of stability of the load-carrying fibers. Strength failure predictions based on point-stress and average-stress criteria,[1] originally developed for tensile loadings, have been used[2-4] for compressive loadings. In the application of the point-stress criterion,[3] for example, compressive failure of the fibers at a predetermined distance from the hole boundary under the action of longitudinal stress along the fiber is assumed. While the point-stress criterion was originally formulated on a laminate basis, it has since been applied ply-by-ply.[5] Despite its tempting simplicity, the point-stress criterion does not provide insight into the local material behavior and does not relate the local behavior to the failure process. The failure of composite materials is generally complex and micromechanically governed. It is important that the physical characteristics of the actual failure process be reflected by an appropriate model.

A microbuckling failure criterion[6,7] is a step in rationalizing compressive failure based on the micromechanics of the material. It can be applied to the principal load-carrying fibers at a point in a similar fashion as the point-stress criterion. Microbuckling has been shown to be a critical failure mode for composites with a highly flexible matrix material. For practical composites with a high modulus resin, such as graphite/epoxy, microbuckling occurs at load values much higher than observed in experiments.[7] Moreover, similar to the recent applications of the point-stress failure criterion,[3,4] the microbuckling criterion assumes the failure to be the result of unidirectional stresses along the fiber direction. It is suspected, however, that shearing stresses, either induced by the presence of a discontinuity or resulting from externally applied loads, may affect the compressive failure.

Presented as Paper 86-1017 at the AIAA/ASME/ASCE/AHS 27th Structures, Structural Dynamics and Materials Conference, San Antonio, TX, May 19-21, 1986; received June 30, 1986; revision received Jan. 2, 1987.

*Assistant Professor, Engineering Science and Mechanics. Member AIAA.

†Professor, Aerospace and Ocean Engineering. Member AIAA.

The experimentally observed shear crippling failure mode[3] (Fig. 1) for plates with a hole is believed to be[8] the result of the kinking failure of the principal load-carrying fibers. Fiber kinking is characterized by a band of buckled and fractured fibers (Fig. 2) in a laminate at a point near a notch, a cutout, or a defect under the action of both shearing and compressive deformations.[9-12] Therefore, a change in the relative magnitudes of the shearing and compressive stresses for different layups may affect the failure load. The effect of shearing stresses may be particularly important for anisotropic laminates or for plates under combined compressive and shearing loads.

The present work is an investigation of a failure model for the in-plane failure of orthotropic and anisotropic plates with a hole under combined in-plane loadings. A model previously developed for the fiber kinking failure of load-carrying plies near a crack[13] under combined local compressive and shear loadings is applied to plates with holes. In addition to the externally applied compressive load, in-plane shear loading is also considered. To demonstrate the model, failure predictions are first compared with available experimental results for quasi-isotropic and orthotropic laminates under axial loading. The applied loading is then extended to a combined axial and shear loading. Predictions are also made for anisotropic laminate configurations, obtained by rotating the principal axis of orthotropy with respect to the load direction.

Failure Model

The failure model presented in this paper includes the effects of local compressive and shearing stresses near a cutout on the failure of load-carrying fibers. These stresses may be the result of externally applied normal loads along the axis of the plate[13] or a result of combined axial and shear loads. The model modifies Rosen's microbuckling model[6] to include the shearing stresses. Individual fibers are modeled as beams on an elastic foundation. The cross section of the fiber beam is rectangular, with a thickness equal to the fiber thickness h and a unit depth. The thickness of the foundation is equal to the distance between the fibers, $2c$ (Fig. 3). Following Rosen,[6] the shearing deformation of the fibers and the extensional deformation of the matrix are neglected. The fiber ends are assumed to remain straight with one end left free to deflect sideways under the action of the side force resulting from the shearing stresses (Fig. 3).

An energy approach is used for the formulation of the equilibrium equation and boundary conditions for the fiber. Taking the first variation of the total energy of the system, the equilibrium equation of the system can be obtained as

$$(E_f I_f v'')'' + \left[P_f - 2cG_m\left(1+\frac{h}{2c}\right)^2\right]v'' = 0 \tag{1}$$

and the general boundary conditions at $x=0$ and $x=\ell$ as either

$$v=0 \text{ or } -(E_f I_f v'')' + \left[2cG_m\left(1+\frac{h}{2c}\right)^2 - P_f\right]v' - qP_f = 0 \tag{2a}$$

and as either

$$v'=0 \text{ or } E_f I_f v'' = 0 \tag{2b}$$

where v is the fiber deformation, E_f and I_f the fiber elastic modulus and first moment of intertia, G_m the matrix shear modulus, P_f the compressive fiber force, ℓ the fiber length, and q the ratio of the side force to the compressive force, $q=S_f/P_f$.

Assuming zero-slope fiber ends, we have, at $x=0$, $v=v'=0$; and at $x=\ell$, $v'=0$ and the force condition of Eq. (2a). The resulting microbuckling load for the fiber is similar to the one obtained from Rosen's model

$$P_{f,C} = 2cG_m\left(1+\frac{h}{2c}\right)^2 + \frac{\pi^2}{\ell^2}E_f I_f \tag{3}$$

except that the second term in the equation is neglected by Rosen, assuming the buckling wave length ℓ to be much larger than the fiber width h. In the present study, buckling wave lengths that lead to failure are expected to be small so that the second term significantly contributes to the critical load. More important, with the present approach, significant lateral displacement of the fiber end is possible at loads substantially smaller than the microbuckling load, even for small local shear stresses. Rosen's model, on the other hand, assumes perfectly straight fibers up to the microbuckling load.

The present model assumes the strength failure, rather than the microbuckling instability, of the fibers of the principal load-carrying lamina. High bending stresses developed at the restrained ends (see Fig. 3) as a result of excessive deformation of the fiber due to side forces are thought to be the cause of the breaking of the fibers that leads to crippling.

As with the point-stress criterion, the implementation of the model calls for the determination of the point where the maximum fiber stress is compared to the allowable fiber stress. It is assumed that the distance r from the cutout or notch boundary to the failure point is a material constant that is independent of the ply combinations and stacking sequence of the laminate. Once the distance is determined, it is necessary to search for a point around the notch or cutout where the combination of axial and shear forces maximizes the fiber stress for the principal load-carrying lamina. In this work, the search is conducted in 1 deg angular increments around the notch. The stresses at each point are transformed to the principal axes of the load-carrying ply. The model is essentially a point-stress criterion, applied on a ply-by-ply basis, that compares the fiber stress resulting from combined local stresses with the fiber strength.

The value of the maximum stress that can be carried by a fiber is not well established in the literature and is assumed here to be 2400 MPa. The value of the fiber length assumed for the model is $\ell=0.05$ mm. This is a representative value for the length of broken fiber fragments observed in Ref. 10. However, predictions of the model were not found to be sensitive to small variations of the fiber length ℓ.

The model is applied to plates with a circular hole. The value of r is determined by using experimental data available in the literature. An analytical approach is used to calculate the stresses around the hole.

For a plate with finite dimensions, the stresses obtained by the given formulation must be corrected for finite size effects. For orthotropic plates, the correction factor is not only a function of the hole size to plate width ($2R/W$) ratio but is also a function of the degree of orthotropy of the material.[15] In the present work, only corrections for finite width from Ref. 15 are applied. Therefore, the examples presented are limited to plates with large length to width ratios.

Failure Predictions

The kinking failure model is first used in an effort to capture the essential features of the available experimental data. For comparison, predictions are also made by using the point-stress criterion of Whitney and Nuismer[1] applied on a ply-by-ply basis using stresses along the fiber direction. Experimental data available in the literature is typically for graphite-epoxy specimens. Representative material properties used for graphite-epoxy are given in Table 1.

Experimental-Prediction Correlation

Experimental values of the far-field failure strains for quasi-isotropic plates with a hole[3] are used to evaluate the value of the distance r from the crack tip to the failure point. The values of $r=1.5$ mm for the kinking model and 1.2 mm for the point-stress model give a good fit to the experimental

Table 1 Unidirectional material properties used

Longitudinal modulus, GPa	131.00
Transverse modulus, GPa	13.00
Shear modulus, GPa	6.40
Major Poisson's ratio	0.38
Thickness, mm/ply	0.14
Fiber volume fraction	0.71
Short beam shear strength, MPa	131.00
Fiber compressive strength, GPa	2.40
Fiber thickness, mm	0.008
Critical fiber length, mm	0.05

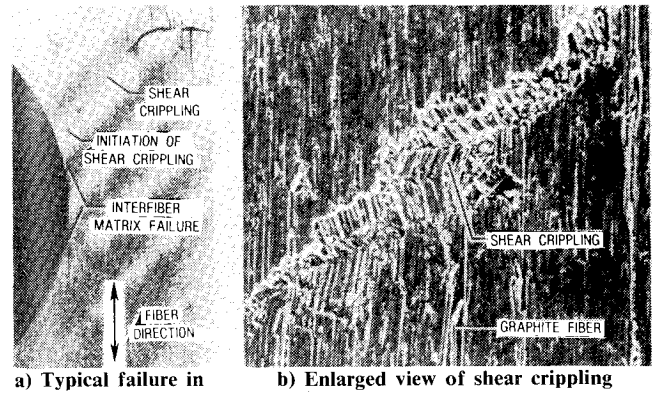

a) Typical failure in a laminate.

b) Enlarged view of shear crippling failure.

Fig. 1 Shear crippling failure of a specimen with a hole, from Ref. 3.

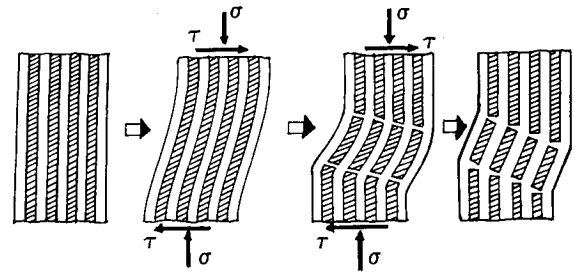

Fig. 2 Kinking mode of compressive failure.

data in Fig. 5. Since r is assumed to be independent to the laminate layup, this value is used for the rest of the results presented. Predictions are also extended to some ±45-deg-dominated plates with a hole (Fig. 5). The present model agrees well with the experimental results. The point-stress criterion, on the other hand, predicts far-field failure strains that are too high for the ±45-deg-dominated plates and requires a different value of either the distance r or the failure stress as the laminate is changed. This is expected because the point-stress criterion is intended for 0-deg dominated laminates only.[3] The failure of the ±45-deg-dominated laminates is affected more than that of the 0-deg-dominated laminates by shearing stresses; therefore, a model that can include the combined effect of shearing and compressive stresses performs better.

The proposed kinking model was also checked against recent experimental results[4] to see the effect of the amount of 0-deg plies in the laminate on failure loads (Fig. 6). Ply orientations for the different laminates used are summarized in Table 2. Predictions made by the present and the point-stress models are based on the same r values that are used in Fig. 5. The point-stress model shows an increased load-carrying capacity as the percent of 0-deg plies is increased. The present predictions made for a percent of 0-deg plies higher than 70% indicate, however, a drop in the load-carrying capacity of the plates. Most of the predictions in the figure are based on the failure of 0-deg plies that are principal load-carrying layers in the laminate. But for laminates with a very small thickness of 0-deg plies, the failure of 0-deg plies may not necessarily mean failure of the plate. The solid and dashed lines with dots on them (extended from 0% 0-deg plies) for small values of the percent of 0-deg layers are obtained by assuming the failure to be in the ±45-deg plies.

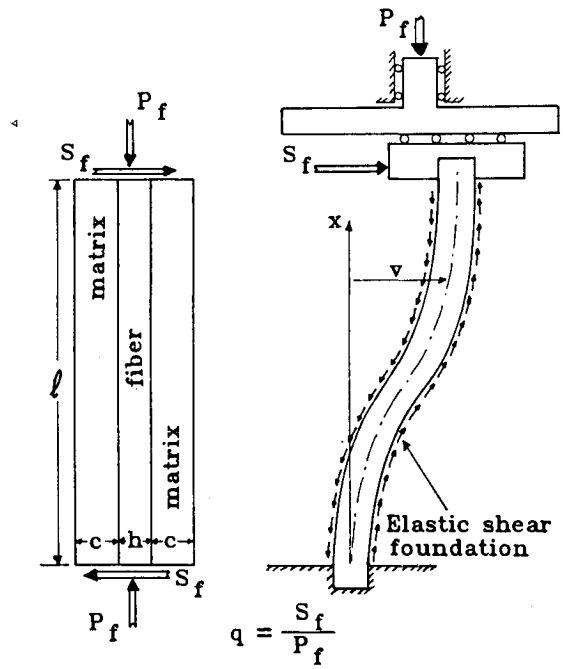

Fig. 3 Beam on an elastic foundation model of a fiber under combined axial and side forces.

Table 2 Ply orientation and thickness of various laminates used for failure predictions

Laminate	Ply orientation	Thickness, mm	0-deg plies, %
A[a]	$0_{12}/\pm45_{12}/90_{12}$	6.72	25.0
B	$\pm45_{36}/90_6$	10.92	—
C	$0_{12}/\pm45_{30}/90_6$	10.92	15.4
D	$0_{24}/\pm45_{24}/90_6$	10.92	30.8
E	$0_{36}/\pm45_{18}/90_6$	10.92	46.2
F	$0_{48}/\pm45_{12}/90_6$	10.92	61.5
G	$0_{60}/\pm45_6/90_6$	10.92	76.9

[a]From Ref. 3.

Plates Under Combined Loading

Predictions are also made for plates under the combined action of externally applied compressive and shear loadings. For plates under axial compressive force only, the principal load-carrying plies are the 0-deg plies oriented along the loading direction or the plies oriented closest to the axial direction. The determination of the principal load-carrying plies is less obvious in the case of combined loading. Depending on the ratio of the applied compressive force to the shearing force, ±45-deg plies can experience higher compressive stresses than the 0-deg plies. In applying the present model or the point-stress model for laminates with different layups, the ply that gives the lowest failure load is assumed to be the one that controls the failure. However, we must note that the failure prediction based on the first ply failure

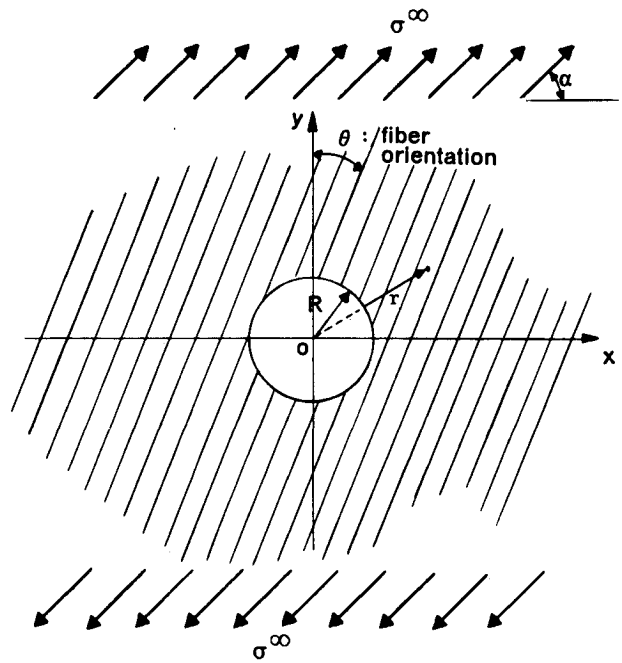

Fig. 4 Infinite plate with an elliptical cutout.

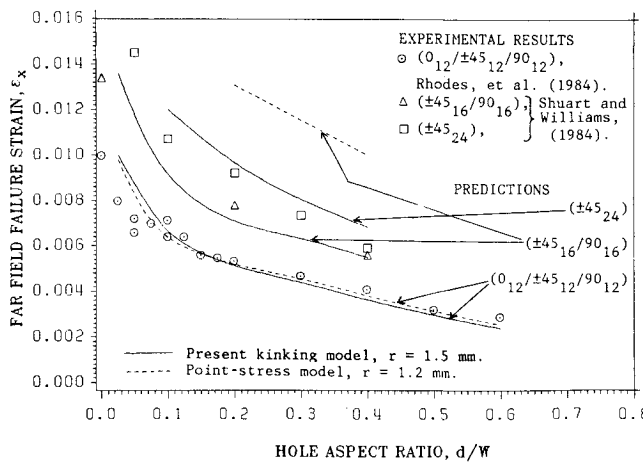

Fig. 5 Compressive failure of plates with a hole.

is not good when the ply carries a small portion of the applied load. Such cases require further investigation of the analytical experimental failure load correlation to determine the plies that are critical for failure. In the present work, for cases where the predictions indicate that plies that do not constitute the majority of the thickness are critical, predictions for the second most critical plies are also presented.

Failure load predictions, obtained by using the point-stress criterion without the effect of local shearing stresses and the present model, are shown in Fig. 7 for a quasi-isotropic plate with a $2R/W$ ratio of 0.1. The failure load is normalized with respect to the failure load of the laminate with no applied shear stress. For small values of the ratio of the shear load to the compressive load, the present model predicts a significant reduction in the load-carrying capacity, whereas the point-stress criterion predicts a negligible effect. For an applied shearing stress equal to half the compressive stress, the present model suggests an almost 30% reduction in failure load. Up to this value of the ratio of the shear stress to the compressive stress, the failure of the plate is governed by the failure of 0-deg plies in the laminate. As the relative magnitude of the shear load is increased beyond half the compressive load, both models suggest the failure to be driven by the failure of ±45-deg plies and the predictions from both models get closer to each other. For shear stress equal to compressive stress, the reduction in the failure load is as much as 45%, and both predictions are within 9% of one another. Similar curves generated by using the present kinking model for different values of the $2R/W$ ratio showed a negligible effect of the hole size on the failure load ratio.

Normalized failure loads predicted by the present kinking model for four laminates, identified by letters from Table 2 (including the one previously dicussed) are compared in Fig. 8 for a $2R/W$ ratio of 0.2. The laminate with only ±45-deg plies, laminate B, is the least sensitive to the presence of the applied shear load. For a ratio of shear to compressive load of 0.5, there is a load reduction of only 20% as compared to 47% for the $0_{48}/\pm 45_{12}/90_6$ F laminate (61.5% 0-deg plies). The change in the failure mode (0-deg or ±45 deg-governed failure) is indicated for each line by a short vertical line segment.

Stress Solution Around a Circular Hole

An elasticity solution[14] for the stresses around an elliptical or circular hole is used, in conjunction with classical lamination theory, to determine the location of the point around the hole at which the combination of compressive and shear stresses will result in fiber failure for the principal load-carrying lamina. The solution assumes an infinitely large homogeneous anisotropic plate with a traction-free elliptical hole. A remote uniaxial stress σ^∞ at an arbitrary orientation α with respect to the x axis is applied to the plate (Fig. 4) at infinity. The stress state at infinity is, therefore,

$$\sigma_x^\infty = \sigma^\infty \cos^2\alpha \quad \sigma_y^\infty = \sigma^\infty \sin^2\alpha \quad \tau_{xy}^\infty = \sigma^\infty \sin\alpha\cos\alpha \tag{4}$$

The stress components near the hole for the problem are[14]

$$\sigma_x = \sigma^\infty \cos^2\alpha + 2Re[s_1^2\Phi_0'(z_1) + s_2^2\Psi_0'(z_2)]$$

$$\sigma_y = \sigma^\infty \sin^2\alpha + 2Re[\Phi_0'(z_1) + \Psi_0'(z_2)]$$

$$\tau_{xy} = \sigma^\infty \sin\alpha\cos\alpha - 2Re[s_1\Phi_0'(z_1) + s_2\Psi_0'(z_2)] \tag{5}$$

where the primes denote the derivatives of the complex potentials Φ_0 and Ψ_0 with respect to the complex arguments z_1 and z_2, respectively; and s_1 and s_2 are the nonconjugate roots of a characteristic equation

$$a_{11}s^4 + 2a_{16}s^3 + (2a_{12} + a_{66})s^2 - 2a_{26}s + a_{22} = 0 \tag{6}$$

which depends on the anisotropic elastic compliance coefficients a_{ij}. The complex variables z_1 and z_2 are defined in the Cartesian coordinates

$$z_1 = x + s_1 y \qquad z_2 = x + s_2 y \tag{7}$$

The derivatives of the complex functions Φ_0 and Ψ_0 for a plate with a hole of radius R are

$$\Phi_0'(z_1) = A_1(\sigma^\infty,\alpha)\left[1 - \frac{z_1}{\sqrt{z_1^2 - R^2(1+s_1^2)}}\right]$$

$$\Psi_0'(z_2) = A_2(\sigma^\infty,\alpha)\left[1 - \frac{z_2}{\sqrt{[z_2^2 - R^2(1+s_2^2)]}}\right] \tag{8}$$

where

$$A_1(\sigma^\infty,\alpha) = \frac{-i\sigma^\infty[(s_2\sin 2\alpha + 2\cos^2\alpha) + i(2s_2\sin^2\alpha + \sin 2\alpha)]}{4(s_1 - s_2)(1 + is_1)}$$

$$A_2(\sigma^\infty,\alpha) = \frac{i\sigma^\infty[(s_1\sin 2\alpha + 2\cos^2\alpha) + i(2s_1\sin^2\alpha + \sin 2\alpha)]}{4(s_1 - s_2)/(1 + is_2)}$$

Anisotropic Plates Under Pure Compression

Failure predictions under pure compressive loads are made for the same set of laminates presented in Table 2 by

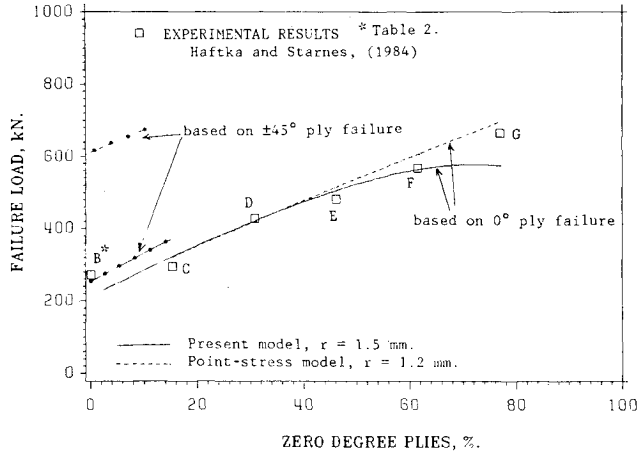

Fig. 6 Compressive failure of plates with different layups.

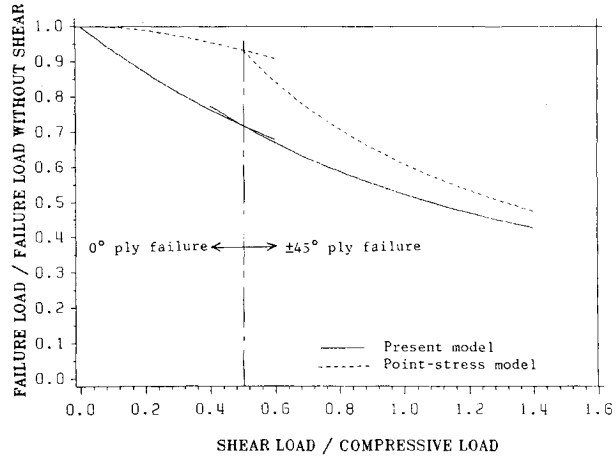

Fig. 7 Effect of shear load on a quasi-isotropic plate.

rotating the principal axis of orthotropy with respect to the loading direction. Because of the anisotropy introduced with respect to the loading axis, applied compressive stresses induce shearing stresses in the plane of the plate. Such laminates may be used for aeroelastic tailoring in aircraft applications.[16] It is expected, however, that such compression shear coupling may result in a more critical stress state around a cutout, which could lead to an early failure. The incoporation of the effect of shearing stresses on failure in the present model allows us to assess the effect of anisotropy.

The effect of shear compression coupling on the compressive failure strength is investigated first for a quasi-isotropic plate. Although isotropic in terms of in-plane stiffness properties, quasi-isotropic laminates demonstrated an anisotropic nature in tensile strength.[17] A reduction observed in strength for off-axis tension specimens is attributed to the interlaminar stresses at the free edge. For the compressive case studied here, change in relative magnitudes of the compressive and shearing stresses around the cutout changed the compressive strength as the laminate was rotated. The ratios of the compressive failure loads of a plate with a quasi-isotropic laminate rotated with respect to the loading axis to that of an unrotated plate (loaded along the 0-deg plies) are given in Fig. 9 for both the present model and the point-stress model. The point-stress model predicts an increase in the failure load as the angle of rotation approaches 22.5 deg, whereas the present model predicts as much as a 10% reduction in the failure load. The difference between the two predictions is entirely due to the inclusion of the shearing stresses around the hole in the present model.

Failure predictions by the present model for some of the orthotropic laminates of Table 2 are summarized in Fig. 10 for a range of angle of rotation from 0 to 45 deg. For laminate F, which has a high degree of orthotropy favoring the applied load direction, the failure load decreases significantly as the plate is rotated. The model predicts failure to occur at the ±45-deg plies (referred to the original layup) when the plate is rotated by more than 5 deg. But for such a small percentage of ±45-deg plies in the laminate, the final failure may be governed by the failure of 0-deg plies. For laminates B and C, which have a high degree of orthotropy favoring the direction perpendicular to the loading direction, the failure load increases as the angle of rotation is increased. Failure is predicted to be governed by the 0-deg plies for most of the range considered.

Although rotating the principal axis of anisotropy of the plate with respect to the loading direction shows a strength reduction under pure compression, it can be used to improve the strength under combined compression and shearing loads. Failure predictions for a plate with laminate F under a combined compressive and shearing load are given in Fig. 11 as the orientation of the 0-deg plies varied. The magnitude of the shearing force is assumed to be equal to half of the applied compressive load. The failure load in the figure is normalized with respect to the failure load of the unrotated plate under pure compression. The load-carrying capacity of the unrotated configuration is reduced by approximately 45% due to the addition of the shear load, which is 50% of the compressive load. By rotating the 0-deg fibers in a direction opposite to the applied shearing load direction, however, the load-carrying capacity of the plate is increased. For a rotation of 22.5 deg, the reduction of the load carrying capacity is only 20% compared to that of unrotated plate in pure compression.

The anisotropic plate configurations discussed herein are assumed to deform freely under the compressive loads. Because of the anisotropic shear-compression coupling, the plate deforms in shear as well as in axial compression, and the loaded edge moves sideways. If the in-plane shear deformation is suppressed in a test by a support fixture at the loaded edge, a shear load is applied at the boundary. The ratio of the shear load to the compressive load would be a function of the angle of rotation of the principal axis of orthotropy with respect to the loading direction. Failure predictions under combined compressive and shearing loads simulating such restraining action are presented. As an approximation, the ratio of the shearing load to the compressive load is calculated for a plate without a hole as the plate is rotated with respect to the compressive loading axis.

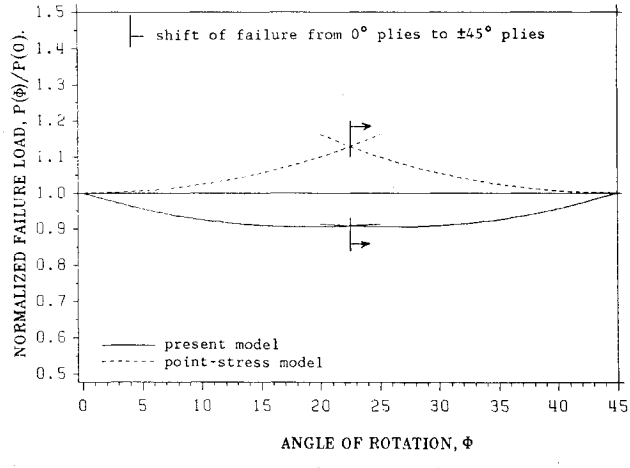

Fig. 9 Compressive strength of a plate with a quasi-isotropic laminate rotated with respect to the loading axis.

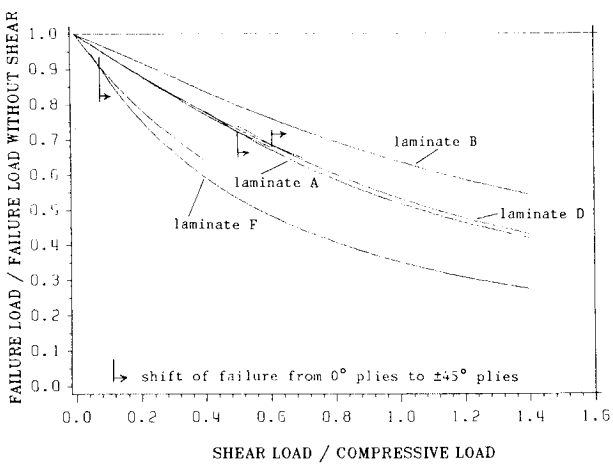

Fig. 8 Effect of shear load on plates with different layups.

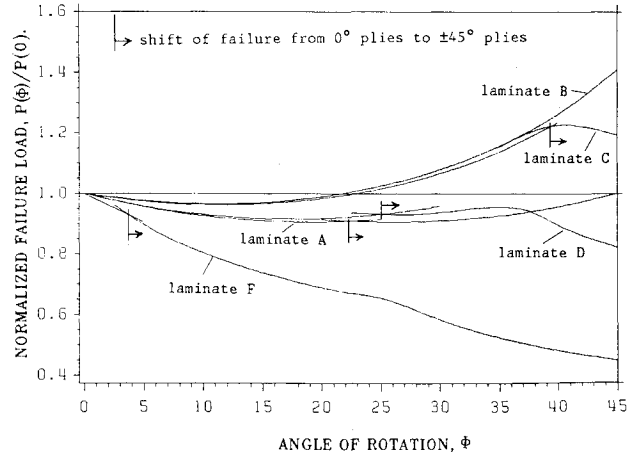

Fig. 10 Comparison of compressive strength of different laminates rotated with respect to the loading axis.

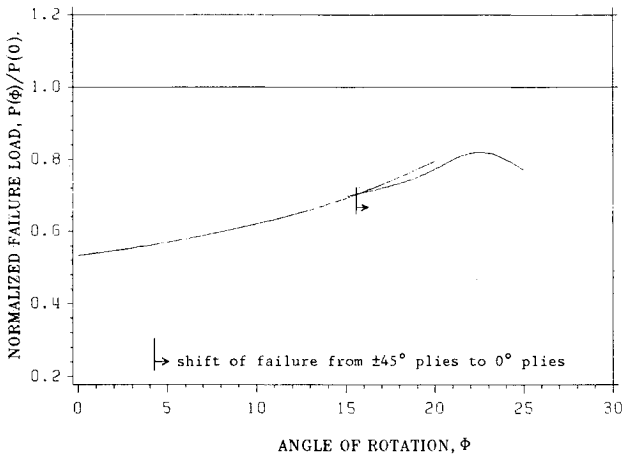

Fig. 11 Compressive strength of a plate with laminate F rotated with respect to the loading axis under combined compressive and shear loading (shear loading 50% of the compression). Failure load is normalized with respect to the unrotated plate without shear.

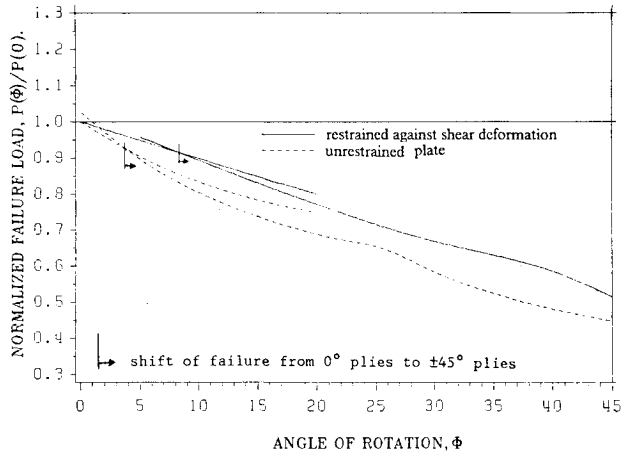

Fig. 12 Compressive strength of a plate with laminate F restrained against shearing deformations and rotated with respect to the loading axis under compressive loads.

The results are compared in Fig. 12 to the predictions without the effect of restraint (dashed line). Clearly, Fig. 12 reveals that the failure load of the plate restrained against shear deformation would be larger than that of the unrestrained plate at the same configuration.

Concluding Remarks

A failure model for the prediction of the compressive strength of plates with a hole is investigated. The model, previously developed and applied for plates with a crack, is based on fiber kinking failure and accounts for the effects of combined shearing and compressive stresses around a hole in a plate. Therefore, the model is applicable to anisotropic plates under combined shearing and compressive loadings. Comparison of the model predictions with the available experimental results for quasi-isotropic and orthotropic plates indicated a good agreement for the kinking failure model.

Predictions for orthotropic plates under combined shearing and compressive loading are compared with predictions of a point-stress model. While the point-stress model predicted only a moderate decrease in load-carrying capacity as compared to a plate loaded only in compression, the fiber-kinking model indicated significant reductions for cases where 0-deg plies are critical.

Predictions based on the kinking and point-stress failure models are made for anisotropic plates obtained by rotating the principal axis of orthotropy of a plate with respect to the loading. When the 0-deg plies governed failure, the two models gave contradictory results. For example, for a quasi-isotropic plate, the kinking model predicted strength reductions, whereas the point-stress model predicted an increase in strength. For a plate with a highly orthotropic laminate in favor of the applied load direction, the failure load decreased significantly as the plate was rotated. For a plate under combined shearing and compressive loads, on the other hand, rotating the principal axis of orthotropy in a direction opposite to the applied shearing load improved the load-carrying of the plate, indicating a potential use of orthotropy for strength improvements for plates with holes.

Acknowledgments

This work was supported by NASA Grant NAG-1-601.

References

[1]Whitney, J. M. and Nuismer, R. J., "Stress Fracture Criteria for Laminated Composites Containing Stress Concentrations," *Journal of Composite Materials*, Vol. 8, July 1974, pp. 253-265.

[2]Nuismer, R. J. and Labor, J. D., "Application of the Average Stress Failure Criterion: Part II—Compression," *Journal of Composite Materials*, Vol. 13, Jan. 1979, pp. 49-60.

[3]Rhodes, M. D., Mikulas, M. M. Jr., and McGowan, P. E., "Effects of Orthotropy and Width on the Compression Strength of Graphite-Epoxy Panels with Holes," *AIAA Journal*, Vol. 22, Sept. 1984, pp. 1283-1292.

[4]Haftka, R. T. and Starnes, J. H. Jr., "Use of Optimum Stiffness Tailoring to Improve the Compressive Strength of Composite Plates with Holes," *Proceedings of the AIAA/ASME/ASCE/AHS 26th Structures, Structural Dynamics and Materials Conference*, Orlando, FL, April 1985, Pt. 1, pp. 426-431.

[5]Garbo, S. P. and Ogonowski, J. M., "Strength Predictions of Composite Laminates with Unloaded Fastener Holes," *AIAA Journal*, Vol. 18, May 1980, pp. 585-589.

[6]Rosen, B. W., "Mechanics of Composite Strengthening," *Fiber Composite Materials*, American Society of Metals, Metals Park, OH, Oct. 1964.

[7]Greszczuk, L. B., "Microbuckling of Lamina-Reinforced Composites," *Composite Materials: Testing and Design (Third Conference), ASTM STP 546*, American Society for Testing and Materials, 1974, pp. 5-29.

[8]Hahn H. T. and Williams, J. G., "Compression Failure Mechanisms in Unidirectional Composites," NASA TM 85834, Langley Research Center, Hampton, VA, Aug. 1984.

[9]Evans, A. G. and Adler, W. F., "Kinking as a Mode of Structural Degradation in Carbon Fiber Composites," *Acta Metallurgica*, Vol. 26, 1978, pp. 725-738.

[10]Berg, C. A. and Salama, M., "Fatigue of Graphite Fiber-Reinforced Epoxy in Compression," *Fiber Science and Technology*, Vol. 6, 1973, pp. 79-118.

[11]Parry, T. V. and Wronski, A. S., "Kinking and Compressive Failure in Uniaxially Aligned Carbon Fibre Composite Tested Under Superposed Hydrostatic Pressure," *Journal of Materials Science*, Vol. 17, 1982, pp. 893-900.

[12]Weaver, C. W. and Williams, J. G., "Deformation of a Carbon-Epoxy Composite Under Hydrostatic Pressure," *Journal of Materials Science*, No. 10, 1975, pp. 1323-1333.

[13]Gürdal, Z., "Automated Design of Composite Plates for Improved Damage Tolerance," Ph.D. Dissertation, Virginia Polytechnic Institute and State University, Blacksburg, VA, Jan. 1985.

[14]Savin, G. N., *Stress Concentration around Holes*, Pergamon Press, Oxford, 1961.

[15]Hong, C. S. and Crews, J. H., "Stress Concentration Factors for Finite Orthotropic Laminates with a Circular Hole and Uniaxial Loading," NASA TP 1469, NASA Scientific and Technical Information Office, 1979.

[16]Lynch, R. W. and Rogers, W. A., "Aeroelastic Tailoring of Composite Materials to Improve Performance," *Proceedings of the AIAA/ASME/SAE 17th Structures, Structural Dynamics and Materials Conference*, King of Prussia, PA, May 1976, pp. 61-68.

[17]Zhou, S. G. and Sun, C. T., "Strength of Quasi-Isotropic Composite Laminates Under Off-Axis Loading," *ASME Winter Annual Meeting, Dec. 1984, ASME Pub. AD-08, pp. 79-85, 1984.*